Clarifying Human White Matter

Brian A. Wandell

Department of Psychology and Stanford Neurosciences Institute, Stanford University, Stanford, California 94305; email: Wandell@stanford.edu

Annu. Rev. Neurosci. 2016. 39:103–28

First published online as a Review in Advance on April 1, 2016

The *Annual Review of Neuroscience* is online at neuro.annualreviews.org

This article's doi: 10.1146/annurev-neuro-070815-013815

Keywords

tractography, connectome, diffusion weighted imaging, dMRI, diffusion spectrum imaging, diffusion tensor imaging, white matter, oligodendrocytes, quantitative MRI

Abstract

Progress in magnetic resonance imaging (MRI) now makes it possible to identify the major white matter tracts in the living human brain. These tracts are important because they carry many of the signals communicated between different brain regions. MRI methods coupled with biophysical modeling can measure the tissue properties and structural features of the tracts that impact our ability to think, feel, and perceive. This review describes the fundamental ideas of the MRI methods used to identify the major white matter tracts in the living human brain.

Contents

INTRODUCTION

Magnetic resonance imaging (MRI) noninvasively measures function and structure in the human brain at millimeter resolution. Because MRI measurements are noninvasive, they provide an opportunity to study the neural basis of human cognition, behavior, and mental health over time and how the brain changes in response to experience and clinical interventions. Thousands of scientists routinely use MRI, and advances in these methods now reveal far more than what we thought possible 25 years ago.

Diffusion MRI (dMRI) and related analysis methods, including tractography, are particularly effective at clarifying the role of human white matter in health and disease. The methods for analyzing and interpreting dMRI are in a period of rapid development as our field learns how to rigorously relate the data to both biological structures and behavior. Even at this early stage, diffusion measurements and analysis methods show that human white matter changes across the life span and responds to experience.

Any new technology requires an investment of time and effort to develop rigorous theoretical methods to interpret the data and relate them to scientific and clinical problems that matter. The excellent progress made on algorithms for interpreting dMRI is evident from the large, active, and technical literature that spans both dMRI and modeling methods, such as tractography. This review introduces the fundamental ideas of dMRI and tractography and serves as an entry point for those who wish to explore the technical literature more deeply and to participate in these exciting new developments.

WHY WHITE MATTER?

The brain's white matter is principally composed of bundles of axons and glia. The axons conduct nerve impulses between neurons, whose cell bodies are in major brain structures, including the cortex, thalamus, hippocampus, and brainstem. During the past 100 years, the overwhelming emphasis in neuroscience has been on the synapse and spike rates, not the bundles of axons and glia that carry the spikes over long distances. Hence, it is worth taking a moment to ask why a neuroscientist or a cognitive scientist might be interested in the properties of the white matter tracts themselves.

One answer begins with the observation that different cortical systems are specialized to perform different biological functions. Many of these specializations must arise from the pattern of long-range cortical connections rather than the local properties of cell bodies, synapses, and dendrites. This is the classic concept of connectionism, usually credited to Wernicke [1874 (1977)]. He argued that most innovations in the neural mechanisms of thought and emotion arise because of the evolution of novel connections, and this hypothesis continues to be relevant nearly 150 years on (Catani et al. 2013; Geschwind 1965a,b). Studies of human white matter are likely to provide insight into the organization of brain systems and the functions they perform.

A second answer begins with the observation that the properties of the brain's white matter tissue correlate with cognitive abilities, decision making, emotional states, and developmental changes (Fields et al. 2014; Gabrieli 2009; Hoeft et al. 2011; Johansen-Berg et al. 2012; Leong et al. 2016; McKenzie et al. 2014; Purger et al. 2015; Sagi et al. 2012; Samanez-Larkin et al. 2012; Sasson et al. 2013; Schnieder et al. 2014; Tavor et al. 2013; Tsang et al. 2009; Wandell & Yeatman 2013; Yeatman et al. 2011, 2012a). The key technologies for measuring human white matter, including dMRI, tractography, and quantitative MRI (qMRI), measure the tissue properties of healthy human brain development. The field has already demonstrated convincingly that human cognition and emotion depend on the integrity of tissue properties within the white matter. Our understanding of brain function will be incomplete until we understand the significance of the pattern of white matter connections and how the properties of white matter tissue impact neural signals.

HUMAN WHITE MATTER

My colleagues remind me from time to time that tools for measuring the nervous systems of rodents, flies, zebrafish, and *Caenorhabditis elegans* are vastly better than the tools for measuring the human brain. It is worth asking, then, Why measure human white matter? I am specifically interested in the human brain, and I am concerned about the ability to translate findings between species. Knowing when the translation between species can be rigorously established is a significant challenge. The recent literature shows that there are no agreed standards that define which results from rodents and other species can be rigorously interpreted with respect to human biology (Nestler & Hyman 2010, Seok et al. 2013, Smith & Dragunow 2014, Takao & Miyakawa 2015). This limits the power of animal models for understanding the topic that interests me: the human mind and brain. For this reason, studying the white matter in humans should be part of our research portfolio.

A great deal has been learned about human white matter during the past two decades. The volume of human white matter is approximately 4×10^5 mm^3 (Zhang & Sejnowski 2000) and comprises 45% of the total cortical volume (Allen et al. 2003, Schüz & Braitenberg 2002). The volume of white matter and gray matter differs greatly among species; for example, the volume of the entire mouse brain is approximately 0.03% of the human brain (Koch & Reid 2012, table 1),

and mouse white matter comprises less than 10% of its cortical volume. The large difference in scale brings to mind that Anderson (1972) famously titled his analysis of reductionism in physical science "More is Different"; I am convinced that his observation applies to neuroscience.

In humans, the longest white matter fibers are those in the callosal tract, connecting the two hemispheres, and the very-long-range axons deep within the white matter; together, these comprise approximately 4% of the volume of human white matter. The majority of axons make much shorter connections between nearby cortical regions (Schüz & Braitenberg 2002). The ability of axons to carry signals depends on the health of their cell bodies and the nearby glia, including both the oligodendrocytes, whose extensions wrap the axons and form the myelin sheath, and the microglia, which attend to basic immunological processes essential for signal communication (Hanisch 2002).

The coupling of diffusion with qMRI methods that assess tissue properties has had some success in measuring specific features of the white matter axons, including axon diameter (Assaf & Basser 2005; Assaf et al. 2008; Barazany et al. 2009; De Santis et al. 2012, 2014; Huang et al. 2015) and the ratio of the myelin sheath thickness to axon diameter (Purger et al. 2015, Rushton 1951, Stikov et al. 2011). These fundamental tissue properties limit the signaling capabilities of individual axons. These properties may also influence to what extent the signals in nearby axons influence one another, perhaps by synchronizing electrical activity (Damasio & Carvalho 2013, Reutskiy et al. 2003). There are many potential mechanisms of such interaction, including the fact that a single oligodendrocyte wraps multiple axons, and even the possibility of electrical interactions. As one would expect of a living system, the tissue properties of these axons change during development, in response to experience, and across the life span (Lebel et al. 2008, 2012b; Mezer et al. 2013; Wandell & Yeatman 2013; Yeatman et al. 2014a).

CONNECTOMES

Most cortical neurons form synaptic connections only with other nearby neurons; most of these local signals are never communicated to other parts of the brain. But the signals from some neurons are carried on axons that leave the cortical sheet and enter into the white matter. These signals have a special status in that they communicate the results of local computations to other parts of the brain.

Adjacent neuronal cell bodies often project axons in bundles that traverse the white matter together, arriving at a similar destination. These small bundles, usually called fascicles, are sometimes grouped into larger pathways within the core of the white matter that are called tracts. These larger bundles are assigned a name that includes the Latin term for bunch, which is fasciculus [e.g., superior longitudinal fasciculus (SLF); arcuate fasciculus].

A large tract, such as the SLF, can include many fascicles, but not all of these fascicles traverse the full length of the tract. In some cases, say in the optic tract or the optic radiation, there are many fascicles that extend the length of the entire tract. But in other cases, say in the SLF, many fascicles enter and exit at different points. A common metaphor for these pathways is a highway; the fascicles, like vehicles, enter and exit the highway (tract) at different points. Furthermore, the fascicles and tracts sometimes cross through one another.

Tractography algorithms estimate the fascicles from dMRI data. The computational representation of a fascicle is often called a streamline. The term estimated fascicle (eFascicle) would also be appropriate. Tractography algorithms create streamlines whose orientations match the local diffusion orientation. In addition, the algorithms follow principles that ensure the streamlines reflect the general anatomical features of brain fascicles. For example, the end points of streamlines are located in brain structures containing cell bodies (cortex, thalamus, brainstem). The fascicles

are constrained within the white matter; they must not pass through the ventricles or outside the brain. Like brain fascicles, the streamlines do not loop back on themselves, nor are they permitted to curve sharply. Thoughtful algorithms have proposed procedures for estimating fascicles from the dMRI data that are subject to these types of constraints (see the section titled Tractography Algorithms). Beyond following these general principles, tractography algorithms require the setting of specific parameters. For example, the maximum fascicle curvature is a typical parameter; a range of permitted streamline lengths is another typical parameter.

The complete set of streamlines generated by whole-brain tractography is called a connectome (or a tractome or a projectome). A connectome is a model of the white matter fascicles. The streamlines in modern connectomes capture the geometric features of the brain fascicles. The visualizations of streamlines can be compelling (**Figure 1**), sometimes making it hard to remember that these streamlines represent only the geometry of a model and that even the most elaborate connectomes model only a small number of the properties of the underlying biology. For example, there is no representation of the nearby glia or the vasculature or the surrounding fluid. The complexity and molecular richness of modern cellular measurements are phenomenal and extend to the nanometer scale (**Figure 1**). There is much ongoing work aimed at extending the scope and accuracy of the connectome models, and this is discussed in the section titled Validation (Accolla et al. 2014, De Santis et al. 2016, Lutti et al. 2014, Mezer et al. 2013, Stikov et al. 2011, Stuber et al. 2014, Yeatman et al. 2014a, Zhang et al. 2012).

Human neuroimaging estimates fascicles and tissue properties at roughly millimeter resolution. The connectome models are approximations of the full complexity of the underlying tissue, and the strengths and weaknesses of these approximations depend on the algorithms used. There is no consensus on a single best algorithm or even the best parameters for a specific algorithm. We know that different algorithms produce significantly different estimates (Bastiani et al. 2012, Parizel et al. 2007, Takemura et al. 2016a), and further, we know that changes in the parameters of a single algorithm can produce different results. This review describes the choices for producing connectome models and the tools available to evaluate those models.

THE DIFFUSION MRI SIGNAL

The most basic MRI signal (proton density) measures the number of spins (hydrogen nuclei in free water) within a small volume. The general principle of MR is that the instrument excites these spins to produce a signal, and the spin excitation signal decays over time. The MR instrument can be programmed in a variety of ways that influence which interactions with the brain substrate cause the signal to decay.

For diffusion, the MRI instrument is programmed so that the random displacements of the spins attenuate the signal. Moreover, the size of signal attenuation can be measured in each direction by applying appropriate magnetic field spatial gradients. Signal attenuation in a particular direction, θ, is measured by the apparent diffusion coefficient [$A(\theta)$] (Le Bihan & Johansen-Berg 2012, Stejskal & Tanner 1965). Specifically, suppose that the signal from a voxel is S_0 when no diffusion gradients are used. When we apply the spatial gradients and measure, the signal is attenuated by an amount that depends on the direction of the gradient, so that $A(\theta)$ is related to signal attenuation by the equation:

$$S(\theta, b)/S_0 = \exp[-b\,A(\theta)].$$

The variable b groups together a set of physical constants and experimental parameters. These include the strength and duration of the magnetic field gradients. The b-value depends on a

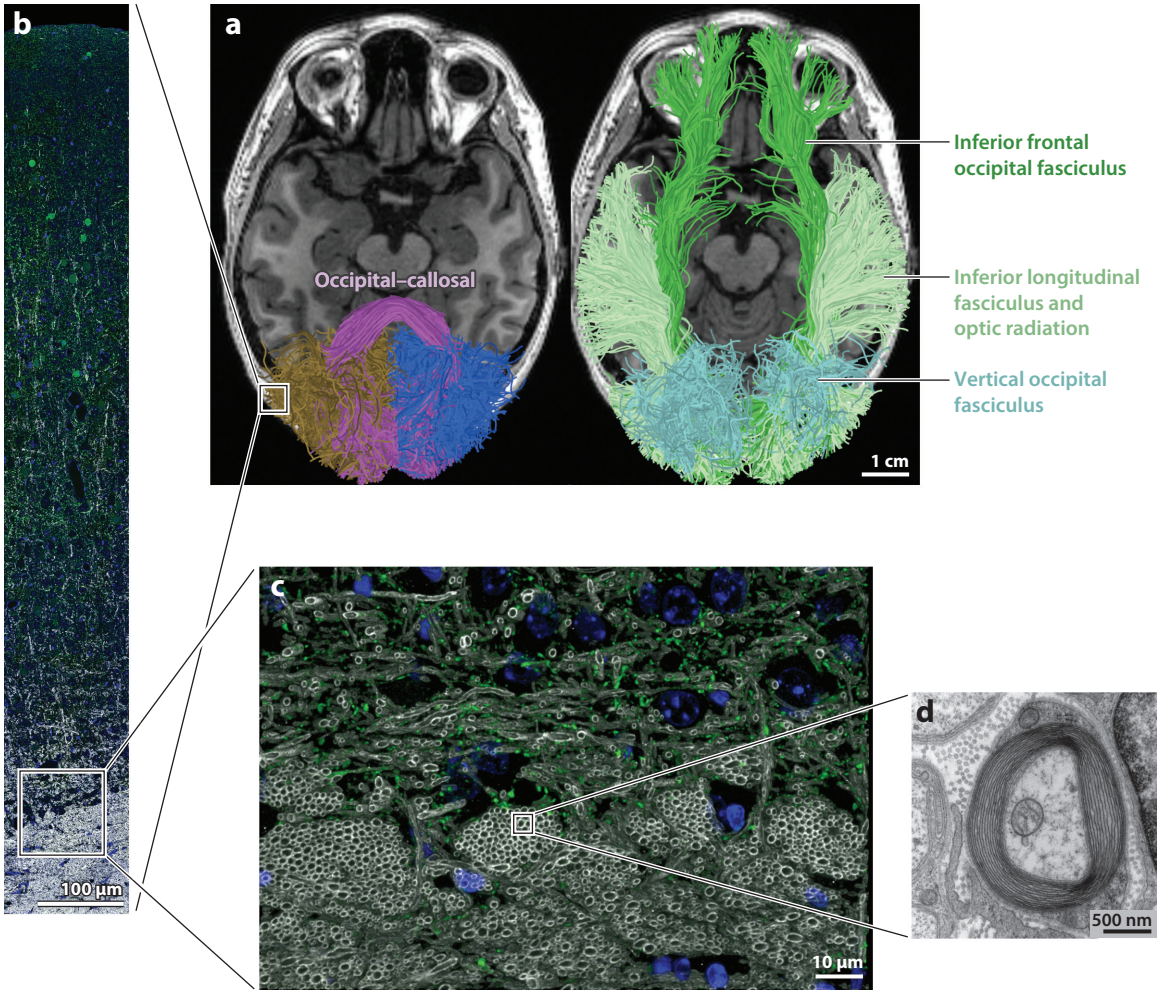

Figure 1

White matter measurements across spatial scales. (*a*) Tractography estimates fascicles at millimeter resolution. The organization of large numbers of estimated fascicles (streamlines) is shown. Streamlines with both end points in the occipital lobe are shown as brown, blue, and purple on the left. The inferior frontal occipital fasciculus, inferior longitudinal fasciculus, optic radiation, and vertical occipital fasciculus are shown in the image on the right. (*b*) Measurements at the micrometer scale reveal a multitude of additional structures and local connections. This image shows a thin strip through the cortex from the pia mater to the white matter (about 140 µm wide and 1 mm high). Of course, measurements at this scale are also models that do not represent finer structures. (*c*) For example, myelin sheaths around individual axons can be identified at the submicrometer scale, which shows the border between the white matter (*lower*) and layer 6 (*upper*) (approximately 130 µm wide and 90 µm tall). These histological images show myelin by basic protein immunostaining (*white*), nuclei by DAPI staining (*blue*), and GABA by immunostaining (*green*). (*d*) The histological images, too, are abstractions that coarsely approximate the molecular organization found within cells at the nanometer scale. For example, at this scale the darkened ring shows the bilipid membranes of the oligodendrocytes that form the myelin wrapping an axon. The scales in this figure span six orders of spatial linear scale, and the abstraction at each scale clarifies certain aspects of the brain architecture; no single scale captures all of the important biological information. I thank Kristina Micheva and Stephen Smith for sharing the histological images and Rosemary Le for preparing the tractography images.

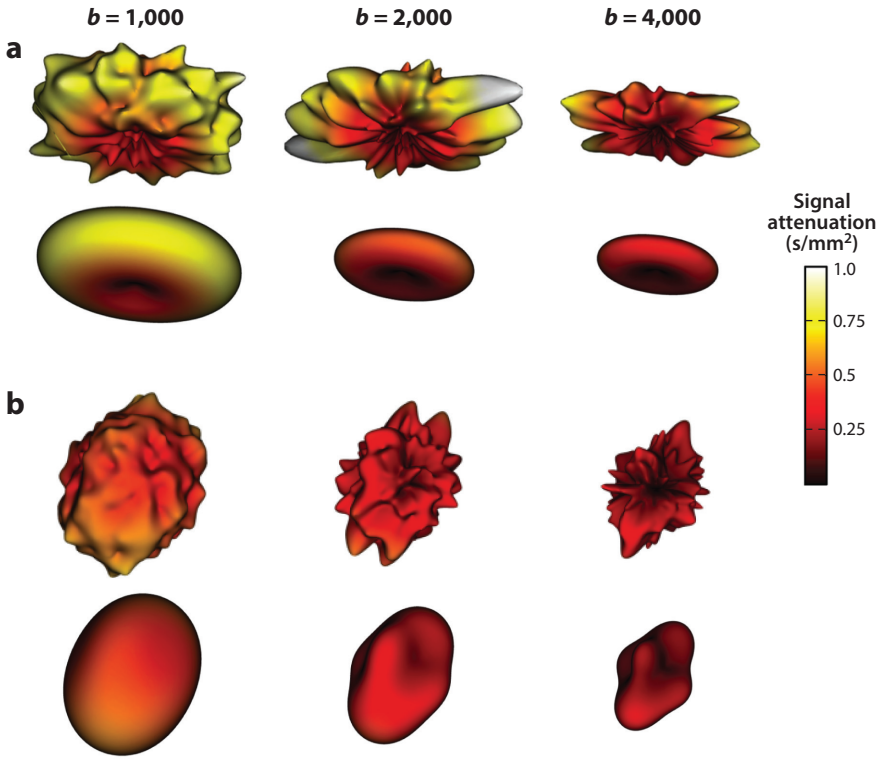

Figure 2

Representation of magnetic resonance signal attenuation caused by diffusion. The surfaces represent measurements and models for 96 different gradient directions. (*a*) The top row shows data from a voxel in the corpus callosum, where the fibers are oriented mainly in the same direction. The bottom row shows the diffusion tensor model fitted to the data. The directions with heavily attenuated signals show the principal direction of these callosal axons. The diffusion tensor model predicts the values in an independent set of measurements better than test–retest. This suggests that the many little ripples in the surface are largely measurement noise. (*b*) A similar set of data is shown from a voxel in the centrum semiovale; this region contains many crossing fibers. The next row shows the ball and stick model fitted to the data. Each column shows data from a different *b*-value. At low *b*-values, only a single principal direction is estimated. At higher *b*-values, the model contains two regions with low values, suggesting that there are crossing fibers in this voxel. The diffusion tensor model cannot capture crossing fibers. Figure adapted from Rokem et al. (2015); calculations can be replicated using these online Jupyter Notebooks: **https://github.com/vistalab/osmosis/blob/master/doc/paper_figures/**, **https://github.com/vistalab/osmosis/blob/master/doc/paper_figures/Figure1.ipynb**, and **https://github.com/vistalab/osmosis/blob/master/doc/paper_figures/Figure7.ipynb**.

combination of experimental parameters (such as gradient strength and gradient duration). Although measurement conditions are generally summarized by a single *b*-value, two scans with the same *b*-value but different combinations of gradient strength and duration measure different tissue properties. This principle is used to good effect in some of the MRI experimental methods described in the section titled Experimental Measurement Choices.

Tractography has its origins in the observation that signal attenuation depends substantially on the orientation distribution of the local axon bundles. **Figure 2** shows the attenuation for a voxel in the corpus callosum, where the fibers are highly directionally coherent (**Figure 2*a***), and

a voxel at the confluence of multiple tracts within the centrum semiovale (**Figure 2*b***). The figure also illustrates how signal attenuation increases as the *b*-value increases.

The change in diffusion signal attenuation with orientation is called the diffusion orientation distribution function (dODF). The underlying fiber orientation distribution function (fODF) is estimated from the dODF using one of several models described in the section titled Diffusion MRI Signal Modeling and Statistical Validation.

Experimental Measurement Choices

When measuring for tractography, one must decide on many experimental parameters, including the number of *b*-values and number of gradient directions. The three dimensions defined by the *b*-values and directions are collectively called *q*-space. The experimentalist selects parameters based on the goals and experimental conditions (e.g., equipment and subjects). A number of papers offer advice on acquisition issues (Campbell & Pike 2014, Jones & Cercignani 2010, Jones et al. 2013, Parker et al. 2013, Tournier et al. 2013).

In practice, it is common to choose a single *b*-value and to measure in 30–60 directions. Acquisitions made with a single *b*-value are called single shell because in the three-dimensional *q*-space each *b*-value defines a sphere (shell). When only a small number of measurements are made on a single shell, the data are usually summarized using a diffusion tensor model. When many directions are measured, the acquisition is called high angular resolution diffusion imaging (HARDI), and more complex models are used. The ability to resolve fascicles oriented in different directions improves as the *b*-value increases. Unfortunately, the signal-to-noise ratio declines with increasing *b*-value, so there is an inherent trade-off between signal-to-noise and angular resolution.

The question of how many different samples and shells to measure is a scientific judgment. The Human Connectome Project sampled *q*-space at three different shells (*b*-values = 1,000, 2,000, and 3,000 s/mm^2) and in approximately 90 directions for each shell (Human Connectome Project 2014, Sotiropoulos et al. 2013). Sampling on multiple shells is called both multishell and Q-BALL imaging (QBI) (Tuch 2004). Sampling at many *q*-space points on a regular three-dimensional grid is called diffusion spectrum imaging (DSI) (Tuch et al. 2003, Wedeen et al. 2000). The number of samples in DSI studies ranges, typically, on the order of 256–512.

People have strong opinions about what you should do. Tournier et al. (2013) have recommended that, to make effective use of their fiber tractography methods, measurements should be taken at a single *b*-value near 3,000 s/mm^2 and in approximately 45 directions. Pestilli et al. (2014, supplemental figure 4) supported this observation, showing that the number of statistically reliable fascicles measured at 2,000 s/mm^2 saturates at approximately 40–60. However, Lebel et al. (2012a) have shown that as few as six directions are sufficient for analyses that aim to locate only the largest tracts. Changing the acquisition parameters also changes which tissue structures determine the attenuation. For example, as the gradient strength or diffusion time increases, structures of different size influence the signal (Stanisz et al. 1997), and this can be used for a purpose: Experimental measurements varying both gradient strength and diffusion time form the basis of efforts to estimate features of the underlying tissue, including axon size and the fanning of axonal arbors and dendrites (Assaf & Basser 2005; Assaf et al. 2008; De Santis et al. 2012, 2014; Zhang et al. 2012). As models advance, DSI sampling will be used to infer fascicle properties in addition to local fiber orientation, such as axon diameters and the thickness of the myelin sheet. But combining these methods is not yet standard practice.

Two other important variables are the voxel size and the amount of time required to obtain the scan. There is extensive work on methods that measure with smaller voxel sizes, down to 1 mm isotropic and smaller. The human connectome data are at 1.25 mm isotropic. There continues to

be active exploration of diffusion measurements with high mean field strength, gradient strength, high spatial and angular resolutions, and using postmortem tissue (Amunts et al. 2013, Foxley et al. 2014, Miller et al. 2011, Seehaus et al. 2015). But the vast majority of scans in the literature are of at least eightfold greater volume (2 mm isotropic).

Recently developed techniques have significantly shortened the measurement time. These technologies measure multiple slices (Feinberg & Setsompop 2013), reducing measurement time by more than half for equal signal-to-noise. Finally, diffusion measurements are being carried out in combination with other methods for studying the properties of white matter tissue. There is hope that the contributions of the different methods can be thoughtfully combined to form a better and more complete assessment of white matter tissue (Axer et al. 2011, Bartzokis et al. 2012, Caspers et al. 2015, Leuze et al. 2014, Magnain et al. 2015, Yeatman et al. 2014a).

Diffusion MRI Signal Modeling and Statistical Validation

Streamlines (or eFascicles) are derived from the diffusion signals in individual voxels. Typically, the derivation begins with a model of the diffusion within the voxel. There are three general approaches to modeling the dMRI signal within a voxel.

The diffusion tensor model treats diffusion as an anisotropic Gaussian process (Basser & Jones 2002, Filler 2009). This leads to a mathematical formulation based on tensors and gives rise to the term diffusion tensor imaging (DTI). The tensor model uses six parameters to describe the Gaussian diffusion within each voxel. The DTI formula also gives rise to several simple, useful scalar statistics (mean diffusivity, radial diffusivity, axial diffusivity, fractional anisotropy).

Initially, it had been hoped that at the spatial scale of individual voxels (2 mm isotropic) human white matter might generally comprise fascicles in a single direction. Were this true, the principal diffusion direction might correspond to the direction of these fascicles. At present, this view has no defenders and many critics. There is nearly universal agreement that the orientation of the ellipse is not a good measure of fascicle orientation in a voxel.

Nonetheless, under many conditions, particularly *b*-values at or below 1,000 s/mm^2, the tensor model approximates the measurements extremely well. Even authors who strongly favor other models use the tensor as a convenient phenomenological description of the data and a means of setting up certain calculations (Tournier et al. 2013). Further, if one simply wants to compare signal attenuation at similar locations in two brains, the tensor model provides an excellent summary of the data and the tensor parameters provide a simple parameterization for comparing the signals.

The ball and stick model predicts signal attenuation as a weighted sum of terms: an isotropic term (ball) and a weighted sum of anisotropic terms (sticks). This parameterization separates the relatively free diffusion of water (ball) and the restricted diffusion imposed by the local cell membranes (sticks). There are several variants of this model. For example, the sticks can be modeled as very thin or as having some thickness (tubes). Often, the diffusion model of a stick is estimated empirically, using data from a region in the brain that comprises only coherently oriented fibers, such as the corpus callosum. Also, some authors include multiple balls in an attempt to characterize different isotropic pools within structures that have different diameters (Daducci et al. 2015, Lemkaddem et al. 2014). Here, I use the general ball and stick metaphor because none of these variants changes the basic concepts of tractography.

Conceptually, there are two approaches for estimating the number and direction of the sticks and the size of the ball, although there have been many different implementations (Behrens et al. 2007, Cook et al. 2006, Daducci et al. 2015, Ferizi et al. 2015, Garyfallidis et al. 2014, Lemkaddem et al. 2014, Rokem et al. 2015, Tournier et al. 2004). In one approach, ball and stick statistical models fit the fiber orientations (Behrens et al. 2007, Rokem et al. 2015). In a second approach, the

fiber orientations are estimated using a spherical harmonic representation of the diffusion data, known as constrained spherical decomposition (Alexander et al. 2002; Frank 2002; Tournier et al. 2007, 2008). These two approaches are not in conflict: It is a matter of choosing to fit the data in the space domain or in the spherical harmonics domain.

The principal output of ball and stick models is the fODF (the distribution of the stick orientations). This is an unwieldy representation and, consequently, some univariate statistics have been proposed, such as generalized fractional anisotropy (Tuch et al. 2003), hindrance modulation (Dell'Acqua et al. 2013), and the dispersion index (Rokem et al. 2015). Consensus on useful univariate statistics may be important to achieve widespread use in scientific and clinical applications.

Both the diffusion tensor model and the ball and stick models fit the signal attenuation data and cross-validate well (Rokem et al. 2015). Cross-validation tests predict a second, independent measurement much better than test–retest reliability. The diffusion model predicts the data better than test–retest reliability in 97% of the voxels, and the ball and stick model predicts the data better in 99.9% of the voxels (Rokem et al. 2015). Hence, both models are a better description of dMRI signal attenuation than the raw data, presumably because the fits eliminate instrumental noise.

How closely do the number, orientation, and dispersion of the sticks reflect the number, orientation, and dispersion of fascicles within a voxel? For certain measurements—those at relatively low gradient strengths ($b = 800$ s/mm^2)—the angular resolution of the measurements is low and the ability to resolve fascicles at slightly different orientations is poor. As the gradient strength increases (say, $b = 3{,}000$ s/mm^2), the angular resolution increases, and it is possible to clearly resolve some fascicles with sufficiently different orientations. These algorithms cannot resolve all local fascicles, but the success of tractography in identifying well-known tracts is good evidence that the estimates provide reliable guidance about the largest fascicles within each voxel.

The term model-free dMRI is generally associated with DSI and QBI: "[DSI is a] model-free diffusion MRI technique . . . without the need for a priori information or ad hoc models" (Wedeen et al. 2005, p. 1385). What is meant is that the diffusion data are collected using a range of b-values and directions without any formal model (tensor, ball and stick) of the signal attenuation function. The signal attenuation levels are interpolated, and the result is the dODF. (Although, of course, interpolation is a simple model.)

Models quickly come into play when investigators determine the fODF from DSI data. In early papers, the fODF was estimated as the peaks in the dODF ["The QBI map is rendered as [a] multicuboid field where the cuboids represent the peaks of the ODF within that voxel" (Tuch et al. 2003, p. 888, figure 2), which is surely a model]. An explicit fiber estimation method (diffusion deconvolution) has been introduced (Yeh et al. 2011).

For both the tensor and ball and stick models, the model predicts an independent data set (cross-validation) more accurately than using the first data set as a prediction of the independent data (test–retest reliability) (Rokem et al. 2015). The excellent predictive ability of the model suggests that a model-free dODF is not an advantage. Rather, the model descriptions are valuable because they combine the data into a summary that reduces the impact of instrumental noise.

TRACTOGRAPHY ALGORITHMS

Tractography algorithms combine dMRI voxel data to estimate relatively long fascicles (streamlines). Each streamline is a model of a biological fascicle that traverses the white matter carrying information between cortical regions. Taken as a whole, these streamlines make up the connectome and are a model of the geometry of the white matter tracts.

In many algorithms, the search for streamlines begins by setting seed points at specific white matter or gray matter locations. For each seed point, the algorithm generates one or more

streamlines. Sherbondy et al. (2008a, 2009) have suggested a number of principles that we might expect to find in a tractography algorithm. These are:

1. Symmetry. If an algorithm starts at a seed location S1 and finds a streamline to location S2, then we expect that starting at S2 the algorithm should be equally likely to find a streamline to S1.
2. Independence. The likelihood of a path between S1 and S2 should depend on data near the path and not on data remote from the path.
3. Data prediction. The collection of streamlines comprising a connectome is a model derived from the diffusion data. The connectome model should, in turn, predict these dMRI data.
4. Physical realizability. The streamlines in the connectome should be consistent with the constraints of physical realizability. For example, the volume of streamlines in a voxel must fit within the voxel.

First Generation

The first tractography models estimated one streamline at a time without accounting for the properties of the complete connectome. These algorithms were deterministic and used the principal direction of the Gaussian diffusion (tensor model) as an estimate of the local fiber direction. Despite their limitations, these algorithms yielded useful estimates of the larger tracts (Conturo et al. 1999, Lazar et al. 2003, Mori & van Zijl 2002, Mori et al. 1999). The ability to find such tracts noninvasively in the living human brain was appropriately met with enthusiasm by many.

The outline of a typical deterministic algorithm is straightforward. Start in a seed voxel. Calculate the diffusion tensor in that voxel. Extend the streamline path along the principal orientation of the tensor in both directions by some step size, say 0.5 mm. Compute the tensors at the new path positions; this might require interpolating among diffusion data at nearby voxels. Decide whether to take another step. There are several reasons you might stop. If the orientation of the tensor at the new position is unclear, stop. If the path is turning too sharply, stop. If the path has exited the white matter, stop. Otherwise, carry on until the two end points of the fascicle are within the gray matter. Then, start again, beginning with a seed at a slightly different location. Even such a simple, deterministic algorithm requires the selection of parameters (stopping criteria, number of seeds to sample), and these choices have a significant impact on the streamlines and, thus, the connectome.

The algorithms generally satisfy the properties of symmetry and independence. But the algorithms are local and greedy, so they never assess whether the connectome model as a whole predicts the data or whether the model satisfies basic physical realizability constraints. Greedy algorithms can produce connectome models with properties that are quite implausible, such as the estimated fascicle densities (Sherbondy et al. 2009).

Second Generation

Many authors have observed that using the principal direction of the diffusion tensor as a summary of the fiber orientation is a poor model. Most obviously, there is no possibility of accurately representing crossing fibers within a voxel, and these crossing fibers are likely widespread (Jeurissen et al. 2013). Further, deterministic tensor-based algorithms do not account for uncertainty in the data. These objections prompted the development of probabilistic tractography methods using dMRI voxel models that allow for multiple fiber directions and also account for measurement uncertainty. An important feature of probabilistic algorithms, which distinguishes them from deterministic, is how the path is traced. Rather than precisely following the peak directions of the

fODF, probabilistic algorithms take steps in a direction that is a random variable around these directions.

Behrens and colleagues (Behrens et al. 2003, 2007; FMRIB Software Library 2015) conceived and implemented tractography algorithms using ball and stick models. These algorithms rely on Bayesian inference mechanisms for deciding how to extend the fascicles. The focus of this implementation is not the tracts themselves, but rather the gray matter end points and cortical connections. This algorithm also includes a derived parameter (connection probability), which is the ratio of the number of tracts between S1 and S2 and the total number of tracts from S1. This statistic fails the principle of independence because the connection probability between S1 and S2 depends on fascicles that have nothing to do with the path between S1 and S2 (Friman & Westin 2005, Sherbondy et al. 2008a). Intuitively, suppose that S1 projects to S2 and S3, but S2 projects only to S1. In that case, the connection probability violates symmetry: The connection probability from S2 to S1 will be much higher than the connection probability from S1 to S2, even though the data along the path between them are the same. The connection probability measures the chance of diffusing from S1 to S2, and because of the branch to S3, this chance may not be the same as diffusing from S2 to S1. The connection probability should not be used as a proxy for connection strength between two gray matter locations.

Tournier et al. (2012) used similar tractography principles but a different computational strategy. They estimated the dODF of a single fascicle using a spherical harmonic representation. They approximated the dODF as a truncated set of spherical harmonics, and they estimated the fODF from the approximation. Their probabilistic tractography algorithm starts with the fODF estimates. In their clear explanation, Tournier et al. (2012) highlight the fact that choosing different parameters and algorithms produces very different results (**Figure 3*a***). Similarly, Feinberg & Setsompop (2013) have pointed out that estimates vary depending on acquisition parameters (**Figure 3*b***).

The same limitations can be found in many types of measurements, including electrophysiology and anatomical tracer studies, which are sometimes described as a gold standard. For example, significant sampling bias occurs depending on the size (resistance) of microelectrodes (Stone 1973). Similarly, history teaches us that there can be significant problems interpreting histological data (Gould 2007, Gould et al. 1999, Rakic 2002), and the differences in estimates of the fundamental properties of white matter based on histology in animals remain large (Jbabdi et al. 2015). These are important issues that the field of tractography is beginning to confront (Takemura et al. 2016a), and this topic is addressed more fully in the section titled Third Generation.

Tract Identification Algorithms

Tractography is sometimes used to estimate tracts and identify connections. But in many applications, we know that a tract is present: For example, we know there is an optic tract in a normally sighted person. Atlases have been created to guide people to the likely identity or location of known tracts (Catani & Thiebaut de Schotten 2008, Hermoye et al. 2004, Wakana et al. 2004, Yeatman et al. 2012b, Yendiki et al. 2011).

Another approach is to develop algorithms to find the most likely path between two locations in individual subjects. Several groups have developed algorithms for finding the most probable path between any two locations (Iturria-Medina et al. 2007, Schreiber et al. 2014, Sherbondy et al. 2008a). These multiple contributions show the need for algorithms that identify specific pathways in individuals.

When we seek to identify a known pathway in the human brain, it is possible to compare tractography with postmortem anatomical methods. Sherbondy et al. (2008b) quantitatively compared

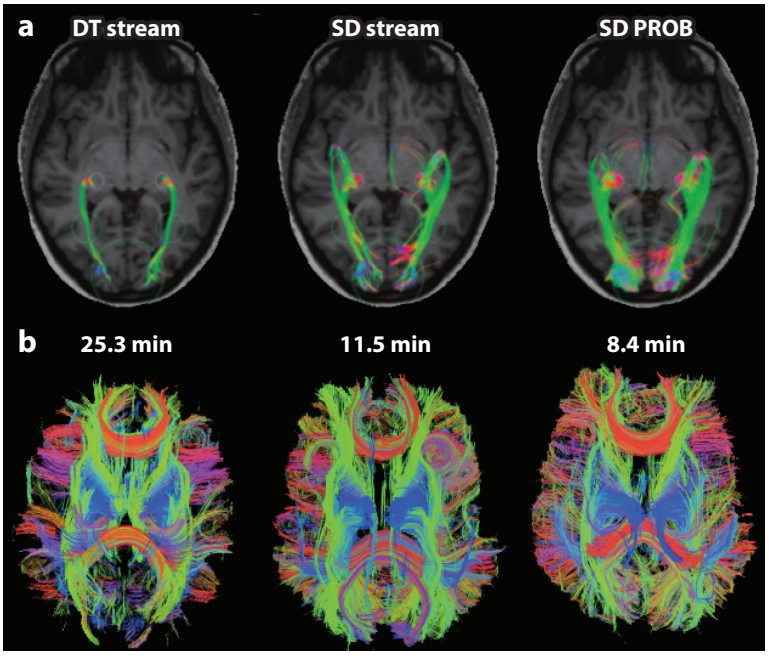

Figure 3

Fascicle estimates depend on the tractography algorithm and magnetic resonance imaging acquisition methods. (*a*) Different algorithms applied to the same diffusion data set generate different streamlines. The three images compare estimates of the optic radiation using a tensor model with deterministic tracking (DT stream), or a spherical deconvolution (SD stream) estimate of the fiber orientation distribution with spherical deconvolution and probabilistic tracking (SD PROB). (*b*) Different acquisition techniques produce different connectomes, even with the same algorithm. The algorithm and acquisition dependences imply that we need methods that decide which estimates are supported by the data. Methods that estimate the confidence intervals given a data set are essential tools for most scientific measurements, and diffusion imaging is no exception. Panel *a* adapted from figure 4 in Tournier et al. (2012). Panel *b* adapted from figure 2 in Feinberg & Setsompop (2013).

the position of key points of the optic radiation measured with tractography and in postmortem analyses, and they found excellent agreement.

Global Tractography

Global tractography describes methods that evaluate connectomes based on the entire set of fascicles with respect to some objective function (Aganj et al. 2011; Daducci et al. 2015; Fritzsche et al. 2012; Jbabdi et al. 2007; Kreher et al. 2008, Lemkaddem et al. 2014; Mangin et al. 2013; Reisert et al. 2011; Sherbondy et al. 2008a, 2009, 2010; Smith et al. 2013, 2015b). The word global is applied both when the algorithm evaluates a whole streamline or the whole connectome; these cases should be distinguished (Pestilli et al. 2014). Here, I concentrate on algorithms for whole connectome evaluation.

Mangin et al. (2002) have presented a range of approaches to global tractography, focusing on an architecture that is motivated by a combination of spin glass theory and spaghetti. The idea of the spin glass is to consider a starting condition as comprising many small line segments that initially cover the white matter volume (spins). An optimization applies simulated forces that bind these

small segments into longer fascicles by adjusting their orientation and number simultaneously to match the diffusion data. The motivation for these forces arises from the authors' thinking about spaghetti—something that I enjoy—although the combination of glass and spaghetti does give one pause.

Reisert et al. (2011) significantly advanced global methods by building a practical algorithm. Their optimization included a method that relies on the ball and stick model for predicting the diffusion data from the collection of fascicles. The optimization uses this forward calculation repeatedly both to form connections among all of the local sticks and to minimize the difference between the connectome and the diffusion data.

Another approach to global tractography is to evaluate the entire set of streamlines with respect to an objective function and then to add and remove entire streamlines, rather than to use segments to build the fascicles. Zhang & Laidlaw (2006) implemented a clear example of this type of global tractography algorithm. They proposed comparing the predicted dMRI signal from all streamlines in a candidate connectome. At first, the set of streamlines predicted a signal that differed from the measurements. They used a sampling procedure to add and remove entire streamlines from the connectome; streamlines were added or removed with the goal of minimizing the difference between the observed and predicted diffusion signals (**Figure 4**).

Sherbondy et al. (2009, 2010) explored a similar method that differs in two ways. First, they noted that many algorithms produced connectomes in which the number of streamlines within different white matter voxels differed by several orders of magnitude. This large dynamic range is inconsistent with the relatively uniform density of the white matter. Thus, Sherbondy et al. (2009) added a constraint to find connectomes with relatively uniform streamline density throughout the white matter, and they expanded the connectome model parameters further in their next paper (Sherbondy et al. 2010). Second, Sherbondy et al. (2009) used a computational architecture that

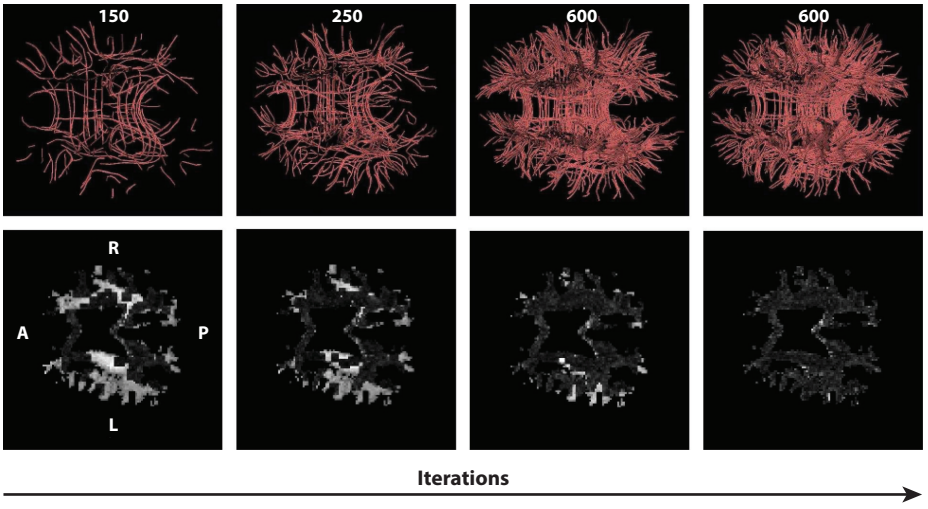

Figure 4

An early global tractography algorithm. The connectome model is used to predict the diffusion data. The decision to add or remove a fascicle is based on the effect the action has on the difference between the predicted and observed signal from diffusion magnetic resonance imaging. The images at the left show the initial stage of this iterative algorithm. The number of fascicles (*inset numbers*) changes over iterations. The difference between the measured and predicted diffusion signals is shown by the grayscale images (*bottom row*). Abbreviations: A, anterior; L, left; P, posterior; R, right. Adapted from Zhang & Laidlaw (2006, figure 2).

separated the process of streamline generation from the process of connectome evaluation. Their algorithm began with a large set of candidate connectomes and then searched for subsets of the connectome that minimized the objective function. As a computational matter, the separation of pathway generation and connectome evaluation still seems like a good idea.

Third Generation

A recent group of algorithms might be considered as a third generation. The new idea is that we have already learned how to produce a wide range of estimated fascicles, and it is even possible that current methods already produce candidate connectomes that include streamlines that are representative of all plausible fascicles. The new algorithms tackle the problem of selecting streamlines from the candidate connectome, mainly by removing streamlines that are either false alarms or repeats of other similar streamlines.

There are two main ideas about how to evaluate the whole connectome and eliminate these unwanted streamlines. Smith et al. (2013, 2015a,b) proposed editing candidate connectomes by evaluating how well the estimated fiber orientation distribution in each voxel matched the streamline orientations in the connectome. In a pair of papers, they proposed methods of editing (filtering) the connectome so that the fiber orientation distribution in the connectome matched the data. They used the word tractogram rather than connectome, and they derived the fODF using spherical deconvolution. Hence, they labeled their approach the spherically informed filtering of tractograms (SIFT). The first implementation of the method filtered by removing fascicles (Smith et al. 2013). The second version added the ability to assign weights to individual fascicles (Smith et al. 2015b).

Daducci et al. (2015) and Pestilli et al. (2014) used a biophysical equation to predict the diffusion data from the connectome model. To fit the connectome to the data, the predicted diffusion from each streamline plus an anisotropic term were added; each streamline contributed some weight that was determined from the fitting procedure.

The two groups use similar mathematical formulations, but they focused on different scientific goals. Daducci et al. (2015) and Lemkaddem et al. (2014) used tractography to link dMRI with tissue microstructure. They argued that the connectome is helpful because in the majority of the voxels the local linear equations between diffusion signals and tissue are underdetermined. The fascicles in the connectome serve as regularizers that guide the interpretation of tissue microstructure in individual voxels.

Pestilli et al. (2014) used tractography to clarify the position of major white matter tracts, and they emphasized methods for evaluating the strength of the evidence in support of specific groups of tracts (Takemura et al. 2016b). They began by observing that the fitting process produced many streamlines with zero weights that do not contribute to the prediction, and these streamlines can be eliminated as false alarms. Surprisingly, as many as 80% of the streamlines have a zero weight in the connectome model and, thus, no empirical support. They went on to develop methods to estimate the strength of support for groups of streamlines with positive weights. They used the methodology to assess the strength of support in the dMRI data in favor of a specific tract, such as the streamlines connecting two cortical locations. The test is based on comparing the error distributions when the streamlines are included versus excluded from the connectome. The statistical techniques build on the linear formula that predicts the diffusion data from the connectome; hence, they call the method linear fascicle evaluation (LiFE).

There is one conceptual difference in the approach used by Smith et al. (2013, 2015a,b) compared with the approach used by Daducci et al. (2015) and Pestilli et al. (2014). Rather than using an objective function that predicts the diffusion data, Smith et al. matched the fiber

orientation distribution, a model that is derived from the diffusion data. I am not sure how well the spherical harmonic approximations do in cross-validation. But if these harmonics cross-validate well, as Rokem et al. (2015) showed for the ball and stick models, this seems like the right approach. Further, the other groups (including my group) should probably minimize error with respect to the model fit rather than the raw data.

Takemura et al. (2016a) added one more twist to the new generation of methods. They observed that, in most cases, users create candidate connectomes using a fixed set of tractography parameters. For example, each choice of the curvature parameter biases the candidate connectome. Takemura et al. (2016a) suggested that a systematic procedure should be applied to create candidate connectomes: Specifically, a set of connectomes created by sweeping out key parameters should be merged. The prediction error that begins with such a candidate connectome (*a*) improves model accuracy and (*b*) includes a more diverse (less biased) set of fascicles. The method builds on LiFE and is called ensemble tractography.

APPLICATIONS TO SCIENCE AND MEDICINE

After only 15 years of development, we can use dMRI and tractography to noninvasively measure white matter structures and tissue properties in the living human brain at millimeter resolution in experiments requiring 10–20 min. The quality of the data and models supports analyses in individuals, making the technique appropriate for clinical applications. These methods are advancing a range of clinical and scientific research projects.

Human Cognition and Clinical Applications

In recognition of the importance of dMRI, the National Institutes of Health supported a project to acquire dMRI data at high resolution from a large number of healthy subjects. These data would enable further processing to specify the human connectome (Van Essen et al. 2012). The project succeeded at providing a high quality, carefully curated, public dMRI data set of the healthy population. These data can be used as a baseline for comparison with subjects studied for other reasons (e.g., a clinical disorder or damage or select behavioral phenotypes).

There is a vast literature describing correlations between white matter tracts and human behavior. This includes the fields of cognition, psychiatry, and neurological disorders (Ameis & Catani 2015, Ben-Shachar et al. 2007, Civier et al. 2015, Fields et al. 2014, Johansen-Berg et al. 2012, Kubicki & Shenton 2014, Mezer et al. 2013, Nordahl et al. 2015, Ogawa et al. 2014, Sagi et al. 2012, Sasson et al. 2013, Schnieder et al. 2014, Tavor et al. 2013, Tsang et al. 2009, Wandell & Yeatman 2013, Wandell et al. 2012, Yeatman et al. 2012a). Advances in applying information technology to combine neuroimaging data from many sites may enable the research from many centers and labs to be assembled into a large and accessible data set (Wandell et al. 2015).

Databases and Tract Profiles

To support the development of tractography, several groups offer tools that analyze the connectomes. There is a set of tools designed to help label the fascicles in a connectome as part of a specific tract. One approach is to label the streamlines based on the voxels it traverses, as specified in a normalized coordinate frame (Calabresea et al. 2015, Hermoye et al. 2004, Lawes et al. 2008, Oishi et al. 2008, Wakana et al. 2004). These atlases are being developed for both human and nonhuman primates. A second approach groups streamlines into tracts based on defining a few criteria, such as their passage through a particular plane or the position in the cortex in the native coordinate frame of the subject (Yeatman et al. 2012b, Yendiki et al. 2011).

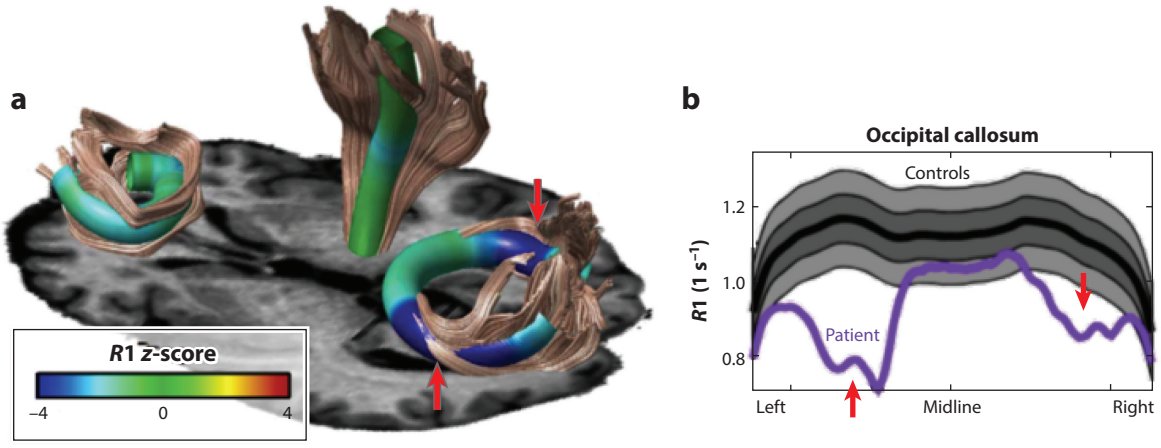

Figure 5

Integrating tractography and quantitative magnetic resonance imaging (qMRI). Tractography localizes white matter tracts using diffusion MRI. (*a*) Quantitative T1 data were collected in healthy controls for each tract at each position. The color overlay on the tracts shows the *z*-scores of the *R*1 (1/T1) data for a single patient with multiple sclerosis. For two of the tracts, the *z*-scores are within the typical range. On the occipital–callosal tract, the *R*1 values are outside of the expected distribution. The data from the occipital–callosal tract are plotted in panel *b*, which shows the mean (*black curve*) and standard deviation (SD) (*gray shaded regions*) lines for a population of age-matched controls. The purple curve shows *R*1 data from this patient. The regions of low *R*1 value likely represent tissue loss. The red arrows point to locations where the *R*1 value differs (3–4 SD) from the control population. Adapted with permission from Yeatman et al. (2014a).

In early analyses, summary measures were provided for some measures (e.g., radial diffusivity), averaged across the entire tract. More recently, papers have included measurements of a diffusion value or another quantitative MRI value assessed along each position of the tract (Yeatman et al. 2012b). Such a tract profile represents the value of either individual streamlines or a summary of the data near the central position of the tract of streamlines (**Figure 5**). This framework is particularly useful for analyzing multimodal data sets; it seems likely that these multimodal data will reveal a great deal about the organization of fibers in the human brain (Bartzokis et al. 2012, Yeatman et al. 2014a).

One aspect of tract profile analysis clearly needs improvement. Currently, we use connectome streamlines to identify voxels in the original data. The tract profiles show a summary of the complete voxel measurements, even though many voxels contain streamlines from several different tracts. We should plot the diffusion prediction from the streamlines of single tracts rather than plotting the values from the raw data.

A second place where we might improve is this: We should strive to develop connectome models that predict both the dMRI and qMRI signals. This advance will take a bit of nerve and some arguing with reviewers, but it will come.

Cellular Biology

There is a natural alliance between scientists studying tissue properties in human white matter and scientists analyzing glia at the cellular level. New results from diffusion and from cell-level measurements all point to the idea that models of white matter and glia will be essential for clarifying how we learn, remember, and feel (Fields 2010, Gibson et al. 2014, Hughes et al. 2013, Long & Corfas 2014, McKenzie et al. 2014, Purger et al. 2015, Sagi et al. 2012). This alliance

is part of a broadening of neuroscience to consider the impact of nonneuronal cells on cognition and behavior (Schnieder et al. 2014). dMRI, qMRI, and tractography can be used noninvasively to study the living human brain and bridge behavior and tissue properties.

VALIDATION

Connectomes are models of white matter. Investigators use these models for at least three different purposes. For some investigators, their primary interest is the matrix of connections between gray matter locations that are defined by the fascicle end points (Hagmann et al. 2008, Sporns 2011, Sporns et al. 2005). The goal of identifying the connections gives rise to the term connectomics. Others are exploring the tissue properties in specific tracts to develop a neuroscience that relates white matter pathways to cognition, emotion, development, or disease (Fitzsimmons et al. 2013, Kubicki & Shenton 2014, Takemura et al. 2016b, Wandell & Yeatman 2013, Wandell et al. 2012, Yeatman et al. 2014b). Yet others are interested in developing biophysical models of tissue properties and using fascicle estimates as regularizers (Daducci et al. 2015). Even when there is a common goal, tractography tools should be selected to serve the experimental conditions. Multiple methods will coexist because different methods are needed for different measurement conditions.

In all cases, we need tools that assess the reliability of our inferences. This is the question of validation, and we can divide validation into three distinct parts. First, measuring parameter reliability can validate models. The connectome model produces many derived parameters (e.g., fascicle density, volume, and orientation; long-range connections; diffusion predictions), and we would like to have some confidence range for the parameter values when we repeat the measurements. Parameter reliability depends on measurement noise, general experimental conditions (e.g., the pulse sequence, field level of the scanner), and biological variability. Bassett et al. (2011) have examined the parameter reliability of connectome models. A number of investigators have examined parameter reliability within voxel diffusion (see Rokem et al. 2015, table 1).

Second, a parameter can be reliable and yet wrong. An algorithm might fit a curve with a straight line. This fit may be stable, but that does not make the curve straight. In this example, parameter reliability is high, but how well the model fits the data (model accuracy) is low. For another example, consider a model that summarizes data with a single parameter, the sample mean. The parameter reliability can be quite good if there are many samples. But the model accuracy will be low if there is significant variance in the data. It is informative to analyze both parameter reliability and model accuracy. This question is not yet part of standard practice in tractography, and I have met scientists who see little value in specifying model accuracy; I find this puzzling.

Third, model parameters may be reliable and the model fit may be excellent, yet the parameters may not correspond uniquely to single biological objects. For example, diffusion signals depend on fiber orientations, but they also depend on the properties of nearby glia, and they may depend on the state of macromolecules that manage protein trafficking. To address parameter validity, we typically turn to methods that pair diffusion with postmortem biological tissue or phantoms (Azadbakht et al. 2015; Dauguet et al. 2007a,b; Fillard et al. 2009, 2011; Neher et al. 2014; Thomas et al. 2014). Even so, I am not optimistic about the central role of such validations, and others have also pointed out that these types of experiments have significant challenges of their own (Jbabdi & Johansen-Berg 2011). A postmortem validation using an animal model on a 7 T scanner would not convince me to accept that the same methods and accuracy apply to data from young children in a 3 T scanner.

The issue of parameter validity came up frequently during the early days of functional MRI (fMRI). Some challenged the value of this signal because it does not correspond uniquely to action potentials (Calford et al. 2005). But such parameter validity is not a prerequisite for having

a valuable measurement; scientists and clinicians can usually make good use of an accurate model that has reliable parameter estimates. With hindsight, it is clear that the quantitative models of the fMRI signal produced much new knowledge about the human brain (Wandell & Winawer 2015, Wandell & Yeatman 2013) even though fMRI captures a mixture of neural signals and has poor parameter validity with respect to action potentials (Logothetis 2008, Logothetis & Wandell 2004). In fact, my reading of the past 25 years is that the fMRI signal opened the field of electrophysiology to be accepting of additional signaling mechanisms, as Bullock and his students (Bullock et al. 2005) had been proposing for many years.

I am not at all opposed to analyzing parameter validity, of course. But I do believe we can learn a great deal and build useful tools based on diffusion even if the model parameters do not match a unique anatomical property at a finer spatial scale. The rigorous development of diffusion and tractography models is advancing our understanding of the human brain and providing helpful clinical advice. Coordinating with equally rigorous models of cognition and emotion and models from medicine will make the field even stronger.

REPRODUCIBLE RESEARCH

Modern tractography software is so complex that a paper describing the software is never capable of capturing the full implementation. An algorithm is reproducible when the author provides an open-source implementation that is well documented and clearly written. The complexity of dMRI and tractography algorithms, combined with the rapid growth of measurement techniques, poses a problem for reproducible science (Buckheit & Donoho 1995, Chan et al. 2014, Donoho 2010). A few paragraphs in a methods section are not enough to permit an independent lab to check a publication for errors, and such checking is fundamental to science. It is time to use software tools for scientific data management that support reproducible research (Marcus et al. 2007, 2013; Scott et al. 2011; Wandell et al. 2015).

CONCLUSIONS

During the next decade, tractography models will include a more comprehensive representation of the biological substrate. The connectome's streamlines will become more complex and include biological tissue properties derived in part from diffusion and also from experiments that combine diffusion with other qMRI measurements. The quantitative measurements may specify axonal size or tissue properties, such as T1, magnetization transfer, or T2 (Assaf et al. 2008; De Santis et al. 2012; Mezer et al. 2010, 2013, 2016; Stikov et al. 2011; Stuber et al. 2014; Weiskopf et al. 2015). Tractography calculations will be one component of a general system that noninvasively characterizes many aspects of white matter structure and tissue properties at submillimeter resolution in the living human brain.

The information we obtain noninvasively from the living human brain is precious, and we have achieved measurements far beyond what students of my generation thought to be possible. Like any technique, there are limitations, but let us take what the terrain will give.

DISCLOSURE STATEMENT

The author is not aware of any affiliations, memberships, funding, or financial holdings that might be perceived as affecting the objectivity of this review.

ACKNOWLEDGMENTS

I thank Michal Ben-Shachar, Joyce Farrell, Rosemary Le, Aviv Mezer, Michael Perry, Ariel Rokem, Hiromasa Takemura, Jon Winawer, and Jason Yeatman for their comments on the manuscript. I gratefully acknowledge the support of the National Science Foundation (grant BCS-1228397) and the Simons Foundation for help with manuscript preparation.

LITERATURE CITED

Accolla EA, Dukart J, Helms G, Weiskopf N, Kherif F, et al. 2014. Brain tissue properties differentiate between motor and limbic basal ganglia circuits. *Hum. Brain Mapp.* 35:5083–92

Aganj I, Lenglet C, Jahanshad N, Yacoub E, Harel N, et al. 2011. A Hough transform global probabilistic approach to multiple-subject diffusion MRI tractography. *Med. Image Anal.* 15:414–25

Alexander DC, Barker GJ, Arridge SR. 2002. Detection and modeling of non-Gaussian apparent diffusion coefficient profiles in human brain data. *Magn. Reson. Med.* 48:331–40

Allen JS, Damasio H, Grabowski TJ, Bruss J, Zhang W. 2003. Sexual dimorphism and asymmetries in the gray–white composition of the human cerebrum. *NeuroImage* 18:880–94

Ameis SH, Catani M. 2015. Altered white matter connectivity as a neural substrate for social impairment in Autism Spectrum Disorder. *Cortex* 62:158–81

Amunts K, Lepage C, Borgeat L, Mohlberg H, Dickscheid T, et al. 2013. BigBrain: an ultrahigh-resolution 3D human brain model. *Science* 340:1472–75

Anderson PW. 1972. More is different. *Science* 177:393–96

Assaf Y, Basser PJ. 2005. Composite hindered and restricted model of diffusion (CHARMED) MR imaging of the human brain. *NeuroImage* 27:48–58

Assaf Y, Blumenfeld-Katzir T, Yovel Y, Basser PJ. 2008. AxCaliber: a method for measuring axon diameter distribution from diffusion MRI. *Magn. Reson. Med.* 59:1347–54

Axer M, Grässel D, Kleiner M, Dammers J, Dickscheid T, et al. 2011. High-resolution fiber tract reconstruction in the human brain by means of three-dimensional polarized light imaging. *Front. Neuroinformatics* 5:34

Azadbakht H, Parkes LM, Haroon HA, Augath M, Logothetis NK, et al. 2015. Validation of high-resolution tractography against in vivo tracing in the macaque visual cortex. *Cereb. Cortex* 25:4299–309

Barazany D, Basser PJ, Assaf Y. 2009. In vivo measurement of axon diameter distribution in the corpus callosum of rat brain. *Brain* 132:1210–20

Bartzokis G, Lu PH, Heydari P, Couvrette A, Lee GJ, et al. 2012. Multimodal magnetic resonance imaging assessment of white matter aging trajectories over the lifespan of healthy individuals. *Biol. Psychiatry* 72:1026–34

Basser PJ, Jones DK. 2002. Diffusion-tensor MRI: theory, experimental design and data analysis – a technical review. *NMR Biomed.* 15:456–67

Bassett DS, Brown JA, Deshpande V, Carlson JM, Grafton ST. 2011. Conserved and variable architecture of human white matter connectivity. *NeuroImage* 54:1262–79

Bastiani M, Shah NJ, Goebel R, Roebroeck A. 2012. Human cortical connectome reconstruction from diffusion weighted MRI: the effect of tractography algorithm. *NeuroImage* 62:1732–49

Behrens TE, Berg HJ, Jbabdi S, Rushworth MF, Woolrich MW. 2007. Probabilistic diffusion tractography with multiple fibre orientations: What can we gain? *NeuroImage* 34:144–55

Behrens TE, Woolrich MW, Jenkinson M, Johansen-Berg H, Nunes RG, et al. 2003. Characterization and propagation of uncertainty in diffusion-weighted MR imaging. *Magn. Reson. Med.* 50:1077–88

Ben-Shachar M, Dougherty RF, Wandell BA. 2007. White matter pathways in reading. *Curr. Opin. Neurobiol.* 17:258–70

Buckheit JB, Donoho DL. 1995. WaveLab and reproducible research. In *Wavelets and Statistics*, ed. A Antoniadis, G Oppenheim, pp. 55–81. New York: Springer-Verlag

Bullock TH, Bennett MV, Johnston D, Josephson R, Marder E, Fields RD. 2005. The neuron doctrine, redux. *Science* 310:791–93

Calabresea E, Badea A, Coe CL, Lubach GR, Stynerd MA, et al. 2015. A diffusion tensor MRI atlas of the postmortem rhesus macaque brain. *NeuroImage* 117:408–16

Calford MB, Chino YM, Das A, Eysel UT, Gilbert CD, et al. 2005. Neuroscience: rewiring the adult brain. *Nature* 438:E3

Campbell JS, Pike GB. 2014. Potential and limitations of diffusion MRI tractography for the study of language. *Brain Lang.* 131:65–73

Caspers S, Axer M, Caspers J, Jockwitz C, Jütten K, et al. 2015. Target sites for transcallosal fibers in human visual cortex—a combined diffusion and polarized light imaging study. *Cortex* 72:40–53

Catani M, Thiebaut de Schotten M. 2008. A diffusion tensor imaging tractography atlas for virtual in vivo dissections. *Cortex* 44:1105–32

Catani M, Thiebaut de Schotten M, Slater D, Dell'Acqua F. 2013. Connectomic approaches before the connectome. *NeuroImage* 80:2–13

Chan AW, Song F, Vickers A, Jefferson T, Dickersin K, et al. 2014. Increasing value and reducing waste: addressing inaccessible research. *Lancet* 383:257–66

Civier O, Kronfeld-Duenias V, Amir O, Ezrati-Vinacour R, Ben-Shachar M. 2015. Reduced fractional anisotropy in the anterior corpus callosum is associated with reduced speech fluency in persistent developmental stuttering. *Brain Lang.* 143:20–31

Conturo TE, Lori NF, Cull TS, Akbudak E, Snyder AZ, et al. 1999. Tracking neuronal fiber pathways in the living human brain. *PNAS* 96:10422–27

Cook PA, Bai Y, Nedjati-Gilani S, Seunarine KK, Hall MG, et al. 2006. *Camino: open-source diffusion–MRI reconstruction and processing.* Presented at Sci. Meet. Int. Soc. Magn. Reson. Med., 14th, Seattle, WA

Daducci A, Dal Palu A, Lemkaddem A, Thiran JP. 2015. COMMIT: convex optimization modeling for microstructure informed tractography. *IEEE Trans. Med. Imaging* 34:246–57

Damasio A, Carvalho GB. 2013. The nature of feelings: evolutionary and neurobiological origins. *Nat. Rev. Neurosci.* 14:143–52

Dauguet J, Delzescaux T, Conde F, Mangin JF, Ayache N, et al. 2007a. Three-dimensional reconstruction of stained histological slices and 3D non-linear registration with in-vivo MRI for whole baboon brain. *J. Neurosci. Methods* 164:191–204

Dauguet J, Peled S, Berezovskii V, Delzescaux T, Warfield SK, et al. 2007b. Comparison of fiber tracts derived from in-vivo DTI tractography with 3D histological neural tract tracer reconstruction on a macaque brain. *NeuroImage* 37:530–38

De Santis S, Assaf Y, Evans CJ, Jones DK. 2014. Improved precision in CHARMED assessment of white matter through sampling scheme optimization and model parsimony testing. *Magn. Reson. Med.* 71:661–71

De Santis S, Assaf Y, Jones DK. 2012. Using the biophysical CHARMED model to elucidate the underpinnings of contrast in diffusional kurtosis analysis of diffusion-weighted MRI. *MAGMA* 25:267–76

De Santis S, Barazany D, Jones DK, Assaf Y. 2016. Resolving relaxometry and diffusion properties within the same voxel in the presence of crossing fibres by combining inversion recovery and diffusion-weighted acquisitions. *Magn. Reson. Med.* 75:372–80

Dell'Acqua F, Simmons A, Williams SCR, Catani M. 2013. Can spherical deconvolution provide more information than fiber orientations? Hindrance modulated orientational anisotropy, a true-tract specific index to characterize white matter diffusion. *Hum. Brain Mapp.* 34:2464–83

Donoho DL. 2010. An invitation to reproducible computational research. *Biostatistics* 11:385–88

Feinberg DA, Setsompop K. 2013. Ultra-fast MRI of the human brain with simultaneous multi-slice imaging. *J. Magn. Reson.* 229:90–100

Ferizi U, Schneider T, Witzel T, Wald LL, Zhang H, et al. 2015. White matter compartment models for in vivo diffusion MRI at 300 mT/m. *NeuroImage* 118:468–83

Fields RD. 2010. Change in the brain's white matter: the role of the brain's white matter in active learning and memory may be underestimated. *Science* 330:768–69

Fields RD, Araque A, Johansen-Berg H, Lim SS, Lynch G, et al. 2014. Glial biology in learning and cognition. *Neuroscientist* 20:426–31

Fillard P, Descoteaux M, Goh A, Gouttard S, Jeurissen B, et al. 2011. Quantitative evaluation of 10 tractography algorithms on a realistic diffusion MR phantom. *NeuroImage* 56:220–34

Fillard P, Poupon C, Mangin JF. 2009. A novel global tractography algorithm based on an adaptive spin glass model. *Med. Image Comput. Comput. Assist. Interv.* 12:927–34

Filler A. 2009. Magnetic resonance neurography and diffusion tensor imaging: origins, history, and clinical impact of the first 50,000 cases with an assessment of efficacy and utility in a prospective 5000-patient study group. *Neurosurgery* 65(Suppl. 4):A29–43

Fitzsimmons J, Kubicki M, Shenton ME. 2013. Review of functional and anatomical brain connectivity findings in schizophrenia. *Curr. Opin. Psychiatry* 26:172–87

FMRIB Softw. Libr. 2015. *FDT UserGuide*. Oxford, UK: Univ. Oxford. **http://fsl.fmrib.ox.ac.uk/fsl/fslwiki/FDT/UserGuide**

Foxley S, Jbabdi S, Clare S, Lam W, Ansorge O, et al. 2014. Improving diffusion-weighted imaging of post-mortem human brains: SSFP at 7 T. *NeuroImage* 102:579–89

Frank LR. 2002. Characterization of anisotropy in high angular resolution diffusion-weighted MRI. *Magn. Reson. Med.* 47:1083–99

Friman O, Westin CF. 2005. Uncertainty in white matter fiber tractography. *Med. Image Comput. Comput. Assist. Interv.* 8:107–14

Fritzsche KH, Neher PF, Reicht I, van Bruggen T, Goch C, et al. 2012. MITK diffusion imaging. *Methods Inf. Med.* 51:441–48

Gabrieli JD. 2009. Dyslexia: a new synergy between education and cognitive neuroscience. *Science* 325:280–83

Garyfallidis E, Brett M, Amirbekian B, Rokem A, Van Der Walt S, et al. 2014. Dipy, a library for the analysis of diffusion MRI data. *Front. Neuroinformatics* 8:8

Geschwind N. 1965a. Disconnexion syndromes in animals and man. I. *Brain* 88:237–94

Geschwind N. 1965b. Disconnexion syndromes in animals and man. II. *Brain* 88:585–644

Gibson EM, Purger D, Mount CW, Goldstein AK, Lin GL, et al. 2014. Neuronal activity promotes oligodendrogenesis and adaptive myelination in the mammalian brain. *Science* 344:1252304

Gould E. 2007. How widespread is adult neurogenesis in mammals? *Nat. Rev. Neurosci.* 8:481–88

Gould E, Reeves AJ, Graziano MS, Gross CG. 1999. Neurogenesis in the neocortex of adult primates. *Science* 286:548–52

Hagmann P, Cammoun L, Gigandet X, Meuli R, Honey CJ, et al. 2008. Mapping the structural core of human cerebral cortex. *PLOS Biol.* 6:e159

Hanisch UK. 2002. Microglia as a source and target of cytokines. *Glia* 40:140–55

Hermoye L, Wakana S, Laurent J-P, Jiang H, Cosnard G, et al. 2004. *White matter atlas*. UCL–JHU. **http://www.dtiatlas.org/**

Hoeft F, McCandliss BD, Black JM, Gantman A, Zakerani N, et al. 2011. Neural systems predicting long-term outcome in dyslexia. *PNAS* 108:361–66

Huang SY, Nummenmaa A, Witzel T, Duval T, Cohen-Adad J, et al. 2015. The impact of gradient strength on in vivo diffusion MRI estimates of axon diameter. *NeuroImage* 106:464–72

Hughes EG, Kang SH, Fukaya M, Bergles DE. 2013. Oligodendrocyte progenitors balance growth with self-repulsion to achieve homeostasis in the adult brain. *Nat. Neurosci.* 16:668–76

Hum. Connect. Proj. 2014. *500 Subjects + MEG2 Reference Manual – Appendix I – Protocol Guidance and HCP Session Protocols*. WU-Minn Consort. NIH Hum. Connect. Proj., Nov. 25. **http://www.humanconnectome.org/documentation/S500/HCP_S500+MEG2_Release_Appendix_I.pdf**

Iturria-Medina Y, Canales-Rodriguez EJ, Melie-Garcia L, Valdes-Hernandez PA, Martinez-Montes E, et al. 2007. Characterizing brain anatomical connections using diffusion weighted MRI and graph theory. *NeuroImage* 36:645–60

Jbabdi S, Johansen-Berg H. 2011. Tractography: Where do we go from here? *Brain Connect.* 1:169–83

Jbabdi S, Sotiropoulos SN, Haber SN, Van Essen DC, Behrens TE. 2015. Measuring macroscopic brain connections in vivo. *Nat. Neurosci.* 18:1546–55

Jbabdi S, Woolrich MW, Andersson JL, Behrens TE. 2007. A Bayesian framework for global tractography. *NeuroImage* 37:116–29

Jeurissen B, Leemans A, Tournier JD, Jones DK, Sijbers J. 2013. Investigating the prevalence of complex fiber configurations in white matter tissue with diffusion magnetic resonance imaging. *Hum. Brain Mapp.* 34:2747–66

Johansen-Berg H, Baptista CS, Thomas AG. 2012. Human structural plasticity at record speed. *Neuron* 73:1058–60

Jones DK, Cercignani M. 2010. Twenty-five pitfalls in the analysis of diffusion MRI data. *NMR Biomed.* 23:803–20

Jones DK, Knosche TR, Turner R. 2013. White matter integrity, fiber count, and other fallacies: the do's and don'ts of diffusion MRI. *NeuroImage* 73:239–54

Koch C, Reid RC. 2012. Neuroscience: observatories of the mind. *Nature* 483:397–98

Kreher BW, Mader I, Kiselev VG. 2008. Gibbs tracking: a novel approach for the reconstruction of neuronal pathways. *Magn. Reson. Med.* 60:953–63

Kubicki M, Shenton ME. 2014. Diffusion tensor imaging findings and their implications in schizophrenia. *Curr. Opin. Psychiatry* 27:179–84

Lawes IN, Barrick TR, Murugam V, Spierings N, Evans DR, et al. 2008. Atlas-based segmentation of white matter tracts of the human brain using diffusion tensor tractography and comparison with classical dissection. *NeuroImage* 39:62–79

Lazar M, Weinstein DM, Tsuruda JS, Hasan KM, Arfanakis K, et al. 2003. White matter tractography using diffusion tensor deflection. *Hum. Brain Mapp.* 18:306–21

Le Bihan D, Johansen-Berg H. 2012. Diffusion MRI at 25: exploring brain tissue structure and function. *NeuroImage* 61:324–41

Lebel C, Benner T, Beaulieu C. 2012a. Six is enough? Comparison of diffusion parameters measured using six or more diffusion-encoding gradient directions with deterministic tractography. *Magn. Reson. Med.* 68:474–83

Lebel C, Gee M, Camicioli R, Wieler M, Martin W, Beaulieu C. 2012b. Diffusion tensor imaging of white matter tract evolution over the lifespan. *NeuroImage* 60:340–52

Lebel C, Walker L, Leemans A, Phillips L, Beaulieu C. 2008. Microstructural maturation of the human brain from childhood to adulthood. *NeuroImage* 40:1044–55

Lemkaddem A, Skioldebrand D, Dal Palu A, Thiran JP, Daducci A. 2014. Global tractography with embedded anatomical priors for quantitative connectivity analysis. *Front. Neurol.* 5:232

Leong JK, Pestilli F, Wu CC, Samanez-Larkin GR, Knutson B. 2016. White-matter tract connecting anterior insula to nucleus accumbens correlates with reduced preference for positively skewed gambles. *Neuron* 89:63–69

Leuze CW, Anwander A, Bazin PL, Dhital B, Stuber C, et al. 2014. Layer-specific intracortical connectivity revealed with diffusion MRI. *Cereb. Cortex* 24:328–39

Logothetis NK. 2008. What we can do and what we cannot do with fMRI. *Nature* 453:869–78

Logothetis NK, Wandell BA. 2004. Interpreting the BOLD signal. *Annu. Rev. Physiol.* 66:735–69

Long P, Corfas G. 2014. Dynamic regulation of myelination in health and disease. *JAMA Psychiatry* 71:1296–97

Lutti A, Dick F, Sereno MI, Weiskopf N. 2014. Using high-resolution quantitative mapping of R1 as an index of cortical myelination. *NeuroImage* 93:176–88

Magnain C, Augustinack JC, Konukoglu E, Boas D, Fischl B. 2015. Visualization of the cytoarchitecture of ex vivo human brain by optical coherence tomography. *Opt. Life Sci., Optics and the Brain 2015, Vancouver, Can.*, pap. BrT4B.5. Washington, DC: Opt. Soc. Am.

Mangin JF, Fillard P, Cointepas Y, Le Bihan D, Frouin V, Poupon C. 2013. Toward global tractography. *NeuroImage* 80:290–96

Mangin JF, Poupon C, Cointepas Y, Riviere D, Papadopoulos-Orfanos D, et al. 2002. A framework based on spin glass models for the inference of anatomical connectivity from diffusion-weighted MR data—a technical review. *NMR Biomed.* 15:481–92

Marcus DS, Harms MP, Snyder AZ, Jenkinson M, Wilson JA, et al. 2013. Human Connectome Project informatics: quality control, database services, and data visualization. *NeuroImage* 80:202–19

Marcus DS, Olsen TR, Ramaratnam M, Buckner RL. 2007. The extensible neuroimaging archive toolkit: an informatics platform for managing, exploring, and sharing neuroimaging data. *Neuroinformatics* 5:11–34

McKenzie IA, Ohayon D, Li H, de Faria JP, Emery B, et al. 2014. Motor skill learning requires active central myelination. *Science* 346:318–22

Mezer AA, Rokem A, Hastie T, Wandell B. 2016. Proton density mapping: ways to remove the receive inhomogeneity. *Hum. Brain Mapp.* In press

Mezer AA, Stikov NA, Kay KN, Dougherty RF, Wandell BA. 2010. *A new quantitative MRI contrast for measuring white matter myelin.* Presented at Soc. Neurosci., 40th, San Diego

Mezer AA, Yeatman JD, Stikov N, Kay KN, Cho NJ, et al. 2013. Quantifying the local tissue volume and composition in individual brains with magnetic resonance imaging. *Nat. Med.* 19:1667–72

Miller KL, Stagg CJ, Douaud G, Jbabdi S, Smith SM, et al. 2011. Diffusion imaging of whole, post-mortem human brains on a clinical MRI scanner. *NeuroImage* 57:167–81

Mori S, Crain BJ, Chacko VP, van Zijl PC. 1999. Three-dimensional tracking of axonal projections in the brain by magnetic resonance imaging. *Ann. Neurol.* 45:265–69

Mori S, van Zijl PC. 2002. Fiber tracking: principles and strategies—a technical review. *NMR Biomed.* 15:468–80

Neher PF, Laun FB, Stieltjes B, Maier-Hein KH. 2014. Fiberfox: facilitating the creation of realistic white matter software phantoms. *Magn. Reson. Med.* 72:1460–70

Nestler EJ, Hyman SE. 2010. Animal models of neuropsychiatric disorders. *Nat. Neurosci.* 13:1161–69

Nordahl CW, Iosif AM, Young GS, Perry LM, Dougherty R, et al. 2015. Sex differences in the corpus callosum in preschool-aged children with autism spectrum disorder. *Mol. Autism* 6:26

Ogawa S, Takemura H, Horiguchi H, Terao M, Haji T, et al. 2014. White matter consequences of retinal receptor and ganglion cell damage. *Investig. Ophthalmol. Vis. Sci.* 55:6976–86

Oishi K, Zilles K, Amunts K, Faria A, Jiang H, et al. 2008. Human brain white matter atlas: identification and assignment of common anatomical structures in superficial white matter. *NeuroImage* 43:447–57

Parizel PM, Van Rompaey V, Van Loock R, Van Hecke W, Van Goethem JW, et al. 2007. Influence of user-defined parameters on diffusion tensor tractography of the corticospinal tract. *Neuroradiol. J* 20:139–47

Parker GD, Marshall D, Rosin PL, Drage N, Richmond S, Jones DK. 2013. A pitfall in the reconstruction of fibre ODFs using spherical deconvolution of diffusion MRI data. *NeuroImage* 65:433–48

Pestilli F, Yeatman JD, Rokem A, Kay KN, Wandell BA. 2014. Evaluation and statistical inference for human connectomes. *Nat. Methods* 11:1058–63

Purger D, Gibson EM, Monje M. 2015. Myelin plasticity in the central nervous system. *Neuropharmacology* In press. doi: 10.1016/j.neuropharm.2015.08.001

Rakic P. 2002. Neurogenesis in adult primate neocortex: an evaluation of the evidence. *Nat. Rev. Neurosci.* 3:65–71

Reisert M, Mader I, Anastasopoulos C, Weigel M, Schnell S, Kiselev V. 2011. Global fiber reconstruction becomes practical. *NeuroImage* 54:955–62

Reutskiy S, Rossoni E, Tirozzi B. 2003. Conduction in bundles of demyelinated nerve fibers: computer simulation. *Biol. Cybern.* 89:439–48

Rokem A, Yeatman JD, Pestilli F, Kay KN, Mezer A, et al. 2015. Evaluating the accuracy of diffusion MRI models in white matter. *PLOS ONE* 10:e0123272

Rushton WA. 1951. A theory of the effects of fibre size in medullated nerve. *J. Physiol.* 115:101–22

Sagi Y, Tavor I, Hofstetter S, Tzur-Moryosef S, Blumenfeld-Katzir T, Assaf Y. 2012. Learning in the fast lane: new insights into neuroplasticity. *Neuron* 73:1195–203

Samanez-Larkin GR, Levens SM, Perry LM, Dougherty RF, Knutson B. 2012. Frontostriatal white matter integrity mediates adult age differences in probabilistic reward learning. *J. Neurosci.* 32:5333–37

Sasson E, Doniger GM, Pasternak O, Tarrasch R, Assaf Y. 2013. White matter correlates of cognitive domains in normal aging with diffusion tensor imaging. *Front. Neurosci.* 7:32

Schnieder TP, Trencevska I, Rosoklija G, Stankov A, Mann JJ, et al. 2014. Microglia of prefrontal white matter in suicide. *J. Neuropathol. Exp. Neurol.* 73:880–90

Schreiber J, Riffert T, Anwander A, Knosche TR. 2014. Plausibility tracking: a method to evaluate anatomical connectivity and microstructural properties along fiber pathways. *NeuroImage* 90:163–78

Schüz A, Braitenberg V. 2002. The human cortical white matter: quantitative aspects of cortico-cortical long-range connectivity. In *Cortical Areas: Unity and Diversity*, ed. A Schüz, R Miller, pp. 377–85. New York: Taylor and Francis

Scott A, Courtney W, Wood D, de la Garza R, Lane S, et al. 2011. COINS: an innovative informatics and neuroimaging tool suite built for large heterogeneous datasets. *Front. Neuroinformatics* 5:33

Seehaus A, Roebroeck A, Bastiani M, Fonseca L, Bratzke H, et al. 2015. Histological validation of high-resolution DTI in human post mortem tissue. *Front. Neuroanat.* 9:98

Seok J, Warren HS, Cuenca AG, Mindrinos MN, Baker HV, et al. 2013. Genomic responses in mouse models poorly mimic human inflammatory diseases. *PNAS* 110:3507–12
Sherbondy AJ, Dougherty RF, Ananthanarayanan R, Modha DS, Wandell BA. 2009. Think global, act local; projectome estimation with BlueMatter. *Med. Image Comput. Comput. Assist. Interv.* 12:861–68
Sherbondy AJ, Dougherty RF, Ben-Shachar M, Napel S, Wandell BA. 2008a. ConTrack: finding the most likely pathways between brain regions using diffusion tractography. *J. Vis.* 8:15.1–16
Sherbondy AJ, Dougherty RF, Napel S, Wandell BA. 2008b. Identifying the human optic radiation using diffusion imaging and fiber tractography. *J. Vis.* 8:12.1–11
Sherbondy AJ, Rowe MC, Alexander DC. 2010. MicroTrack: an algorithm for concurrent projectome and microstructure estimation. *Med. Image Comput. Comput. Assist. Interv.* 13:183–90
Smith AM, Dragunow M. 2014. The human side of microglia. *Trends Neurosci.* 37:125–35
Smith RE, Tournier JD, Calamante F, Connelly A. 2013. SIFT: spherical-deconvolution informed filtering of tractograms. *NeuroImage* 67:298–312
Smith RE, Tournier JD, Calamante F, Connelly A. 2015a. The effects of SIFT on the reproducibility and biological accuracy of the structural connectome. *NeuroImage* 104:253–65
Smith RE, Tournier JD, Calamante F, Connelly A. 2015b. SIFT2: enabling dense quantitative assessment of brain white matter connectivity using streamlines tractography. *NeuroImage* 119:338–51
Sotiropoulos SN, Jbabdi S, Xu J, Andersson JL, Moeller S, et al. 2013. Advances in diffusion MRI acquisition and processing in the Human Connectome Project. *NeuroImage* 80:125–43
Sporns O. 2011. *Networks of the Brain*. Cambridge, MA: MIT Press
Sporns O, Tononi G, Kotter R. 2005. The human connectome: a structural description of the human brain. *PLOS Comput. Biol.* 1:e42
Stanisz GJ, Szafer A, Wright GA, Henkelman RM. 1997. An analytical model of restricted diffusion in bovine optic nerve. *Magn. Reson. Med.* 37:103–11
Stejskal EO, Tanner JE. 1965. Spin diffusion measurements: spin echoes in the presence of a time-dependent field gradient. *J. Chem. Phys.* 42:288–92
Stikov N, Perry LM, Mezer A, Rykhlevskaia E, Wandell BA, et al. 2011. Bound pool fractions complement diffusion measures to describe white matter micro and macrostructure. *NeuroImage* 54:1112–21
Stone J. 1973. Sampling properties of microelectrodes assessed in the cat's retina. *J. Neurophysiol.* 36:1071–79
Stuber C, Morawski M, Schafer A, Labadie C, Wahnert M, et al. 2014. Myelin and iron concentration in the human brain: a quantitative study of MRI contrast. *NeuroImage* 93:95–106
Takao K, Miyakawa T. 2015. Genomic responses in mouse models greatly mimic human inflammatory diseases. *PNAS* 112:1167–72
Takemura H, Caiafa CF, Wandell B, Pestilli F. 2016a. Ensemble tractography. *PLOS Comput. Biol.* 12:e1004692
Takemura H, Rokem A, Winawer J, Yeatman JD, Wandell BA, Pestilli F. 2016b. A major human white matter pathway between dorsal and ventral visual cortex. *Cereb. Cortex* 26:2205–14
Tavor I, Hofstetter S, Assaf Y. 2013. Micro-structural assessment of short term plasticity dynamics. *NeuroImage* 81:1–7
Thomas C, Ye FQ, Irfanoglu MO, Modi P, Saleem KS, et al. 2014. Anatomical accuracy of brain connections derived from diffusion MRI tractography is inherently limited. *PNAS* 111:16574–79
Tournier JD, Calamante F, Connelly A. 2007. Robust determination of the fibre orientation distribution in diffusion MRI: non-negativity constrained super-resolved spherical deconvolution. *NeuroImage* 35:1459–72
Tournier JD, Calamante F, Connelly A. 2012. MRtrix: diffusion tractography in crossing fiber regions. *Int. J. Imaging Syst. Technol.* 22:53–66
Tournier JD, Calamante F, Connelly A. 2013. Determination of the appropriate *b* value and number of gradient directions for high-angular-resolution diffusion-weighted imaging. *NMR Biomed.* 26:1775–86
Tournier JD, Calamante F, Gadian DG, Connelly A. 2004. Direct estimation of the fiber orientation density function from diffusion-weighted MRI data using spherical deconvolution. *NeuroImage* 23:1176–85
Tournier JD, Yeh CH, Calamante F, Cho KH, Connelly A, Lin CP. 2008. Resolving crossing fibres using constrained spherical deconvolution: validation using diffusion-weighted imaging phantom data. *NeuroImage* 42:617–25

Tsang JM, Dougherty RF, Deutsch GK, Wandell BA, Ben-Shachar M. 2009. Frontoparietal white matter diffusion properties predict mental arithmetic skills in children. *PNAS* 106:22546–51

Tuch DS. 2004. Q-ball imaging. *Magn. Reson. Med.* 52:1358–72

Tuch DS, Reese TG, Wiegell MR, Wedeen VJ. 2003. Diffusion MRI of complex neural architecture. *Neuron* 40:885–95

Van Essen DC, Ugurbil K, Auerbach E, Barch D, Behrens TE, et al. 2012. The Human Connectome Project: a data acquisition perspective. *NeuroImage* 62:2222–31

Wakana S, Jiang H, Nagae-Poetscher LM, van Zijl PC, Mori S. 2004. Fiber tract-based atlas of human white matter anatomy. *Radiology* 230:77–87

Wandell BA, Rauschecker AM, Yeatman JD. 2012. Learning to see words. *Annu. Rev. Psychol.* 63:31–53

Wandell BA, Rokem A, Perry LM, Schaefer G, Dougherty RF. 2015. Data management to support reproducible research. arXiv:1502.06900 [q-bio.QM]

Wandell BA, Winawer J. 2015. Computational neuroimaging and population receptive fields. *Trends Cogn. Sci.* 19:349–57

Wandell BA, Yeatman JD. 2013. Biological development of reading circuits. *Curr. Opin. Neurobiol.* 23:261–68

Wedeen VJ, Hagmann P, Tseng WY, Reese TG, Weisskoff RM. 2005. Mapping complex tissue architecture with diffusion spectrum magnetic resonance imaging. *Magn. Reson. Med.* 54:1377–86

Wedeen VJ, Reese T, Tuch D, Weigel M, Dou J, et al. 2000. *Mapping fiber orientation spectra in cerebral white matter with Fourier-transform diffusion MR.* Presented at Proc. Int. Soc. Mag. Res. Med., Denver, CO

Weiskopf N, Mohammadi S, Lutti A, Callaghan MF. 2015. Advances in MRI-based computational neuroanatomy: from morphometry to in-vivo histology. *Curr. Opin. Neurol.* 28:313–22

Wernicke C. 1874 (1977). Der aphasischer Symptomenkomplex: Eine psychologische Studie auf anatomischer Basis. In *Wernicke's Works on Aphasia: A Sourcebook and Review*, transl. GH Eggert, pp. 91–145. The Hague: Mouton

Yeatman JD, Dougherty RF, Ben-Shachar M, Wandell BA. 2012a. Development of white matter and reading skills. *PNAS* 109:E3045–53

Yeatman JD, Dougherty RF, Myall NJ, Wandell BA, Feldman HM. 2012b. Tract profiles of white matter properties: automating fiber-tract quantification. *PLOS ONE* 7:e49790

Yeatman JD, Dougherty RF, Rykhlevskaia E, Sherbondy AJ, Deutsch GK, et al. 2011. Anatomical properties of the arcuate fasciculus predict phonological and reading skills in children. *J. Cogn. Neurosci.* 23:3304–17

Yeatman JD, Wandell BA, Mezer AA. 2014a. Lifespan maturation and degeneration of human brain white matter. *Nat. Commun.* 5:4932

Yeatman JD, Weiner KS, Pestilli F, Rokem A, Mezer A, Wandell BA. 2014b. The vertical occipital fasciculus: a century of controversy resolved by in vivo measurements. *PNAS* 111:E5214–23

Yeh FC, Wedeen VJ, Tseng WY. 2011. Estimation of fiber orientation and spin density distribution by diffusion deconvolution. *NeuroImage* 55:1054–62

Yendiki A, Panneck P, Srinivasan P, Stevens A, Zollei L, et al. 2011. Automated probabilistic reconstruction of white-matter pathways in health and disease using an atlas of the underlying anatomy. *Front. Neuroinformatics* 5:23

Zhang H, Schneider T, Wheeler-Kingshott CA, Alexander DC. 2012. NODDI: practical in vivo neurite orientation dispersion and density imaging of the human brain. *NeuroImage* 61:1000–16

Zhang K, Sejnowski TJ. 2000. A universal scaling law between gray matter and white matter of cerebral cortex. *PNAS* 97:5621–26

Zhang S, Laidlaw DH. 2006. Sampling DTI fibers in the human brain based on DWI forward modeling. *Proc. 28th IEEE EMBS Annu. Int. Conf., New York*, pp. 4885–88. New York: IEEE

Annual Review of Neuroscience

Volume 39, 2016

Contents

Indexes

Errata

An online log of corrections to *Annual Review of Neuroscience* articles may be found at http://www.annualreviews.org/errata/neuro